
Article:
Wang, Chung Yao, Bergström, Edmund, Southgate, Jennifer orcid.org/0000-0002-0135-480X et al. (1 more author) (2022) Surface Shave:Revealing the Apical-Restricted Uroglycome. Journal of Proteome Research. 360–374. ISSN 1535-3893

https://doi.org/10.1021/acs.jproteome.1c00714

A Surface Shave: Revealing the Apical-Restricted Uroglycome

Chung-Yao Wang[1], Edmund Bergström[1,2], Jennifer Southgate[3]‡, Jane Thomas-Oates[1,2b]‡*

[1]Department of Chemistry, University of York, Heslington, York, YO10 5DD, UK

[2]Centre of Excellence in Mass Spectrometry, University of York, Heslington, York, YO10 5DD, UK

[3]Jack Birch Unit, Department of Biology, York Biomedical Research Institute; University of York, Heslington, York YO10 5DD, UK

* j.southgate@york.ac.uk

ABSTRACT This study aimed to investigate the highly-differentiated urothelial apical surface glycome. The functions of the mammalian urothelium, lining the majority of the urinary tract and providing a barrier against toxins in urine, are dependent on the correct differentiation of urothelial cells, relying on protein expression, modification and complex assembly to regulate the formation of multiple differentiated cell layers. Protein glycosylation, a poorly studied aspect of urothelial differentiation, contributes to the apical glycome and is implicated in the development of urothelial diseases. To enable surface glycome characterization, we developed a method to collect tissue apical surface *N*- and O-glycans. A simple, novel device using basic laboratory supplies was

developed for enzymatic shaving of the luminal bladder urothelial surface, with subsequent release and mass spectrometric analysis of apical surface O- and *N*-glycans; the first normal mammalian urothelial *N*-glycome to be defined. Trypsinization of superficial glycoproteins was tracked using immunolabelling of the apically-expressed uroplakin 3a protein to optimize enzymatic release, without compromising the integrity of the superficial urothelial layer. The approach developed for releasing apical tissue surface glycans allowed comparison with the *N*-glycome of total porcine bladder urothelial cells, and thus identification of apical surface glycans as candidates implicated in urothelial barrier function. Data available in MassIve: MSV000087851.

KEYWORDS Bladder, glycome, permethylated glycan, mass spectrometry, tryptic shaving, urothelium.

INTRODUCTION Epithelia are polarised tissues that form interfaces between internal and external spaces. As such, they are highly specialised to perform tissue site-specific functions, such as mucus production and nutrient absorption by the gut, or as barriers against desiccation (skin) or urinary toxicants (urothelium). Being positioned at the interface also provides evolutionary selection for other local features, such as pathogen defence and reception/transduction of external signalling cues. The apical glycome is hence predicted to play a unique role in epithelial tissue-specific interface biology and determining the specific makeup of apical glycan species is prerequisite to understanding this role. Previous studies investigating the polarised glycome have used established epithelial-derived cell lines grown in monolayer culture [1-3] and brain tissue slices [4], but no report has yet characterised an in situ apical epithelial tissue surface.

The urinary bladder is lined by urothelium, a transitional epithelium that forms the tightest epithelial barrier in the body. Urothelium is stratified into basal, intermediate and highly-specialised lumen-facing superficial cells which, as a result of the urothelial differentiation-associated gene expression programme, display unique features that contribute to urinary barrier function. The uroplakins are urothelial differentiation-restricted *N*-glycoproteins that complex to form plaques of asymmetric unit membrane (AUM) in the superficial cell apical membrane that limit transcellular permeability [5]. The complex formation by uroplakins into membrane-inserted plaques is well-characterised and requires precise changes in glycosylation for correct assembly [6, 7]. The apical "uroglycome" has been proposed to further contribute to the functional barrier that defends the urothelium against penetration of toxic substances from the urine and plays a role in defence against adventitious microorganisms in the urine [8-11]. Whilst the apical localisation of specific blood group and other lectin-binding antigens indicates a specific composition, overall the uroglycome remains relatively undefined. In addition to *N*-glycans [10], O-glycans in the form of O-sialoglycoprotein endopeptidase-sensitive mucin glycoproteins have been localised at the luminal surface [12, 13]. A role for glycosaminoglycans (GAGs) in urothelial apical biology has been supported by some [14, 15], but not others [12, 16].

Literature-described approaches to extracellular glycome isolation typically separate cell membranes from whole cell lysates to deliver a preparation enriched in extracellular glycans; however, such a membrane fraction is also likely to contain intracellular glycans due to incomplete separation of the plasma membrane from intracellular membranes. Collecting extracellular glycans from cells with their cell membranes intact avoids this problem and is an essential validation step towards determining the cell surface glycome and its functions. Tryptic shaving is an accepted approach for sampling cell and tissue surface peptides (e.g. [16-18]), but has

found more widespread application in microbes than in mammalian systems, in part due to the physiological effects that proteolysis of cell surface proteins can induce. The team of Blanchard applied tryptic shaving approaches to sample the surface glycans from cultured mammalian cells, using trypsin to release cell surface-exposed glycopeptides, which were retrieved and their glycans released for analysis [1, 3, 19]. Although promising, and acknowledging that the cell membrane needs to remain intact for this method to work, these publications provide no demonstration that the cells do in fact remain intact during the treatment and thus that the glycans released derive only from the plasma membrane as suggested. Nonetheless, given the potential of such an approach, we have scoured the literature for examples where tryptic shaving approaches have been applied to sampling tissue surface glycomes; we have not found any reports of the use of surface shaving approaches to sample the apical glycome from a polarised tissue with specific surface features, such as those of the urothelium.

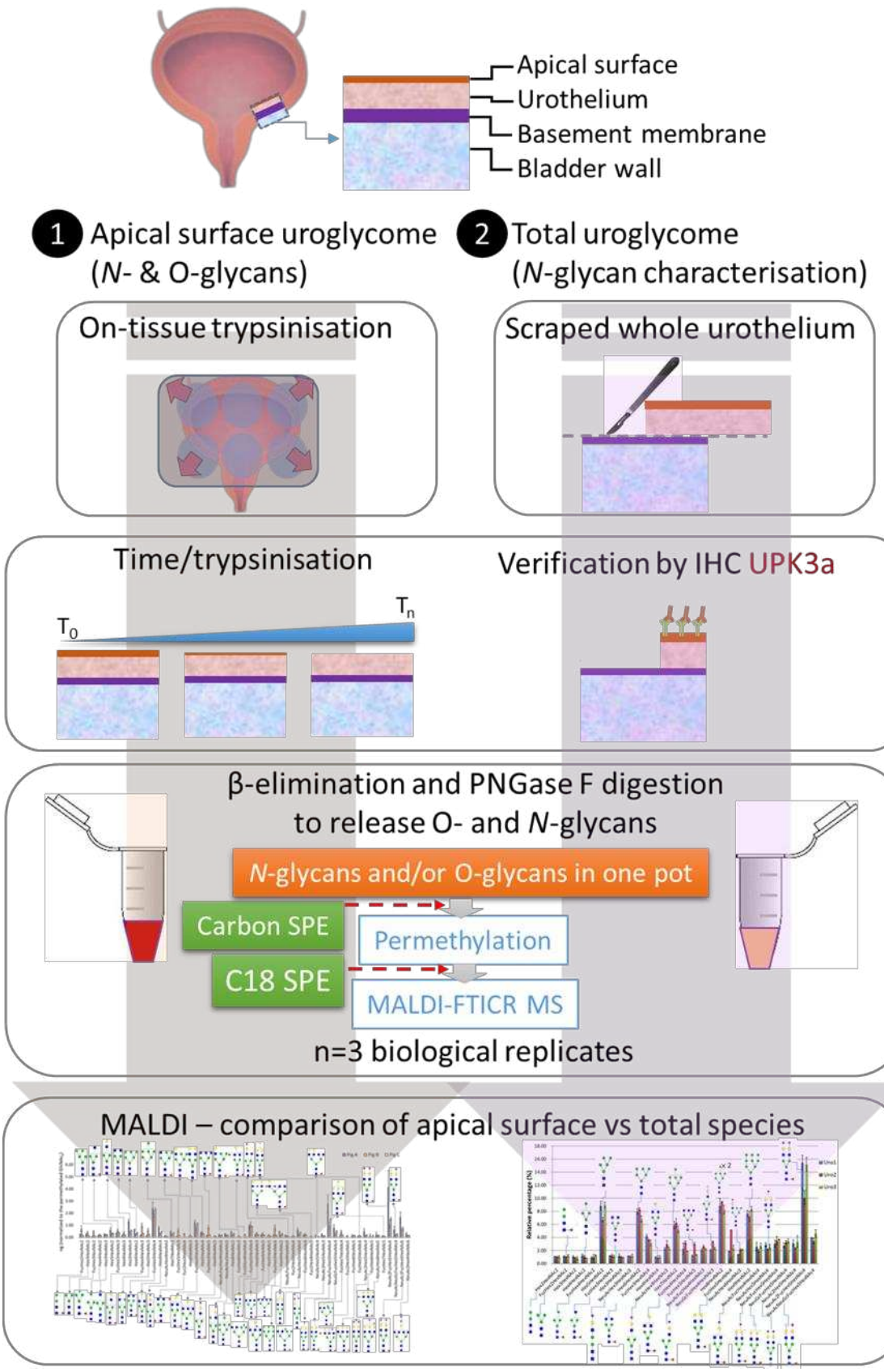
Apical surface
Urothelium
Basement membrane
Bladder wall
1 Apical surface uroglycome
(N- & O-glycans)
2 Total uroglycome
(N-glycan characterisation)
On-tissue trypsinisation
Scraped whole urothelium
Time/trypsinisation
T0
Tn
Verification by IHC UPK3a
β-elimination and PNGase F digestion
to release O- and N-glycans
N-glycans and/or O-glycans in one pot
Carbon SPE
C18 SPE
Permethylation
MALDI-FTICR MS
n=3 biological replicates
MALDI – comparison of apical surface vs total species

Figure 1. Schematic of tissue surface shaving approach for sampling the urothelial apical glycome from abattoir-sourced porcine bladders, alongside whole urothelial cell lysate glycan release and analysis. 1. Tryptic conditions were established to shave the intravesical surface of the urinary bladder. Uroplakin immunohistology was used to ensure that digestion was limited to the apical glycome by monitoring that tryptic digestion removed only the apical glycoprotein layer to release surface-exposed glycopeptides. A method was developed and validated for the release and analysis of the *N*- and O-glycome from these glycopeptides and used to produce the first apical uroglycome of healthy porcine bladder urothelium. 2. Determination of which *N*-glycan species were differentially expressed in the apical glycome required analysis of the whole urothelial tissue glycome, which was developed by harvesting the entire urothelium from the basement membrane before lysis and release of total cell *N*-glycans using the filter-aided *N*-glycan separation (FANGS) approach and permethylation followed by MALDI-MS for semi-quantitative analysis (22). Type IV collagen (Col IV) was used to verify the collection of urothelium without containing the underlying tissues. Semi-quantification of each *N*-glycan species was derived from the normalized signal intensities for each glycan species from triplicate MALDI spots, which were averaged and the mean used to derive the relative percentages of *N*-glycans in one technical replica. The relative percentages of *N*-glycans from three technical replicas were averaged for each biological replica and plotted using Excel; the error bars indicate the standard deviation of the mean. Structures shown are proposed.

Here, we report the development and validation of a novel protocol for apical tissue-surface tryptic shaving to sample and enable description of the urothelial apical glycome. As shown in the schematic (Figure 1), we used abattoir-sourced porcine bladders, as a readily available tissue

with demonstrated similarities to the equivalent human tissue, including expression of uroplakins [20, 21]. To develop a verifiable apical glycome preparation protocol, we established tryptic conditions to digest the luminal intravesical surface of the urinary bladder, using immunodetection of an extracellular domain uroplakin epitope to monitor the success of tryptic shaving and validate that tryptic digestion was limited to the urothelial surface by removing only the apical glycoprotein layer. In this way, we developed optimum conditions for effective release of surface glycopeptides, without extending below or otherwise compromising the tissue surface. Once we had established tryptic shaving conditions that were demonstrated to strip only the apical surface outer layer, we applied them to release surface-exposed glycopeptides. We developed and validated a method for release and analysis of the *N*- and O-glycome from these glycopeptides and have used it in conjunction with glycan profiling approaches that allow relative quantification [22] to produce the first apical "uroglycome" of healthy porcine bladder urothelium. Determination of those *N*-glycan species that were differentially expressed in the apical glycome required analysis of the whole urothelial glycome. For this second arm of the study, we selectively isolated and harvested the entire urothelial tissue compartment, before lysis and release of total urothelial cell *N*-glycans using the filter-aided *N*-glycan separation (FANGS) approach and permethylation followed by MALDI-MS for semi-quantitative analysis [23] and direct comparison with the results of the only other similar study that we are aware of [24]. We further employed immunohistology to the tissue remainder to validate that removal of the urothelium was complete leaving the basement membrane intact.

Here we present our novel approach, validations and results. We discuss the nature and potential functions of the glycans we have shown to be surface-specific and consider how the method could be applied in the future to more precious human urothelial samples in health and disease.

EXPERIMENTAL

Collection of fresh porcine bladders: Fresh porcine bladders were obtained from a local abattoir (A. Traves & Son Ltd, Main Street, Escrick, YO19 6TP, UK) and transported in sealed plastic bags or bottles on ice. Porcine bladders were processed for collecting urothelial cells or conducting on-tissue trypsinization immediately upon receipt by the laboratory.

Tissue fixation and processing for immunohistochemistry: The dissected porcine bladder tissues (<1 cm^3) were fixed in 10% formalin, before routine dehydration through graded ethanols into xylene and embedding into paraffin wax. The antibody used for immunohistochemistry was mouse monoclonal AU1 against UPK3A, a barrier-function-related superficial glycoprotein found on urothelium (Progen Cat No. 651108).

For immunohistochemistry, 5 μm sections were transferred onto glass slides, dewaxed by incubation in xylene, followed by 100 % (v/v), then 70 % (v/v), ethanol, to water and incubated for 10 minutes in fresh 3% hydrogen peroxide to block endogenous peroxidase activity. Heat-induced antigen retrieval was performed by microwave boiling for 10 minutes in 10 mM citric acid buffer (pH 6.0). An avidin biotin block was carried out according to the supplier's instructions (Vector Laboratories) and followed by blocking with 1/10 rabbit serum. Each section was incubated with diluted primary (or control) antibody at ambient temperature for 1 hour, before washing and further incubation with 100 μL biotinylated rabbit-anti-mouse secondary antibody for 30 minutes, followed by washing to remove unbound secondary antibody. Each section was then incubated with 100 μL freshly prepared StrepAB/HRP complex for 30 minutes, rinsed in Tris-buffered saline, then incubated with 200 μL 3,3′-diaminobenzidine solution (Sigma D4293) for 10 minutes, washed with distilled water, followed by staining in

haemotoxylin for 5-10 seconds and washing under the running tap water for one minute. The slides were then dehydrated and mounted with coverslips using dibutylphthalate polystyrene xylene.

On-tissue trypsinisation: The luminal surface of the bladder was gently rinsed twice with 2 mL pre-warmed, sterile Hank's balanced salt solution (HBSS, Gibco Cat# 24020, pH 7.4, 37 °C). Five mg/mL trypsin solution used for conducting on-tissue trypsinization was prepared by diluting 25 g/L trypsin solution (Sigma, Cat#T4549, in 0.9% w/v NaCl, tissue culture grade) with HBSS. One mL of prepared 5 mg/mL trypsin solution was pre-warmed at 37 °C for 5 minutes and added into one of the six reaction vessels, covering the luminal side of the porcine bladder tissue. Trypsinization was carried out for different incubation times at 37 °C. Supernatants were collected and heated to deactivate trypsin at 99 °C for 5 min. Supernatants were subjected to PNGase F digestion and β-elimination sequentially to release *N*- and O-glycans from the same sample solutions. The released glycan pools were purified using solid phase extraction [19] cartridges packed with graphitized carbon (Supelco, Cat#57094). The resulting *N*- and O-glycans were permethylated and purified with using C18 SPE cartridges (Supelco, Cat#57064) prior to MALDI-MS analysis.

***N*-glycan release**: All PNGase F digestions releasing *N*-glycans from samples were carried out with addition of 4 μL of 2 U/μL PNGase F solution (stored in 5 mM potassium phosphate, pH 7.5)(generous gift of Daniel Ungar, University of York, in whose lab this enzyme was produced, as described [25]. All samples were incubated at 37 °C for at least 16 hours.

O-glycan release: β-elimination to release O-glycans from urothelial cell lysates was based largely on the published procedure [24]. 300 μL NH_4OH (28~30%, Sigma-Aldrich) was added into

vacuum-dried samples containing glycopeptides and released *N*-glycans. The resulting solution was sonicated in a sonication bath, temperature controlled at 45 °C, for 5 minutes and then left for 10 minutes. Temperature control of the sonication bath was aided by an external water circulating system maintained at 41-42 °C. The cycle of 5 minutes-sonication/10 minutes-wait was repeated four times to give a total 20 minutes' sonication time and 40 minutes' wait/incubation time.

Carbon SPE method for desalting released glycans: Underivatised glycans released using PNGase F digestion or β-elimination were desalted using carbon SPE cartridges. The sample solution was dissolved in 2 mL HPLC-grade water. The carbon cartridges were sequentially primed with a) 6 mL ACN, b) 6 mL ACN with 0.1% trifluoroacetic acid (TFA), c) 6 mL of HPLC-grade water, d) 6 mL of 50% ACN in HPLC-grade water with 0.1% TFA, e) 6 mL of 5% ACN in HPLC-grade water with 0.1% TFA and f) 6 mL of HPLC-grade water. The sample solution was loaded onto the cartridge and sequentially washed with 2 mL of HPLC-grade water and 1.5 mL of 5% ACN in HPLC-grade water with 0.1% TFA. The glycan fraction was eluted with 3 mL of 50% ACN in HPLC grade water with 0.1% TFA and dried for permethylation.

C18 SPE method for purification of permethylated glycans: This purification of permethylated glycans was only necessary for those glycans produced during on-tissue trypsinization, and was carried out largely as described [26, 27]. The permethylated glycans were dried and reconstituted in 200 µL of MeOH/HPLC-grade water (volume:volume). The C18 cartridges were primed with 6 mL MeOH and followed by 6 mL acetonitrile (ACN). The C18 cartridges were conditioned with 6 mL 100% HPLC-grade water prior to loading the sample solutions. The sample solutions were carefully loaded onto the cartridges and sequentially washed with 5 mL HPLC-grade water, 2 mL 15% ACN in water, 2 mL of 25% ACN in water.

The samples were eluted with 2 mL 50% ACN in water and collected. The collected eluent containing the glycans was dried prior to MALDI-MS analysis.

Filter-aided *N*-glycan separation (FANGS): This procedure was carried out to release *N*-glycans from urothelial whole cell lysates, and was based directly on the published procedure (22) with slight modifications. To make a cell lysate, one vial of collected porcine urothelial cells was heated in SDS lysis buffer (4% w/v sodium dodecyl sulfate, 100 mM dithiothreitol in 100 mM Tris.HCl at pH 7.6) at 95°C in a water bath or a heating block. The cell lysate was mixed well with exchange buffer (8 M urea in 100 mM Tris.HCl pH 7.6) in a ratio of 1:10 cell lysate to exchange buffer by volume. The cell lysate-exchange buffer mixture was transferred into an ultrafiltration device (one filter membrane device with one collection tube; Amicon Ultra-0.5, Ultracel-30 membrane, nominal mass cutoff 30 kDa, Millipore) for centrifugation. The centrifuge was operated at 14,000 x g for 10 min, until all the mixture had passed through the ultrafiltration device. The sample solution retained above the filter membrane was washed twice by the addition of 250 μL of exchange buffer and centrifuged after each. 300 μL of 40 mM iodoacetamide freshly prepared in exchange buffer was then mixed well with the sample solution above the filter membrane and the device left in the dark at ambient temperature for 15 min then centrifuged at 14,000 x g for 10 min. 250 μL of exchange buffer was added into the sample solution above the filter membrane and centrifuged for 10 min. The sample solution above the filter membrane was washed four times with four successive additions of 250 μL of 50 mM ammonium bicarbonate, each followed by centrifugation at 14,000 x g for 10 min. The filter membrane device holding sample solution was transferred to a new collection tube and the sample solution above the membrane mixed with 100 μL of 50 mM ammonium bicarbonate solution and 8 U of PNGase F (2 U/μL). The whole device was sealed with Teflon™ tape and

incubated at 37 °C overnight. After incubation, the digested sample solution was centrifuged first, then washed twice by successive addition of 250 µL of water (HPLC grade) and centrifuged for 10 min after each. The released *N*-glycans were obtained in solution in the collection tube following centrifugation. The released *N*-glycan solution was dried using a vacuum centrifuge.

Permethylation: The permethylation method followed that reported by Ciucanu and Kerek [28], followed here with slight modifications. All samples were vacuum dried in glass reaction tubes prior to permethylation. 1 mL of DMSO (approximately 40 drops) was added into the reaction tube to reconstitute the dried sample. Finely ground NaOH (~10-20 mg) was added to the sample solution, followed by addition of 10 drops of iodomethane (CH_3I). The solution was gently shaken and left to stand for 10 minutes. A further 10 drops of iodomethane were added, vortexed and left to stand for 10 minutes. A final 20 drops of iodomethane were added to the sample solution, again gently mixed, and left to stand for 20 minutes. The reaction was quenched with the slow addition of 1 mL 100 mg/mL sodium thiosulfate solution. 1 mL dichloromethane (DCM) was added into the sample solution, and vortex mixed, to extract the permethylated glycans. The (upper) aqueous layer was removed and the organic layer was washed with 2 mL of HPLC-grade water, repeating four times. The organic layer containing the permethylated glycans was dried using vacuum centrifugation, for subsequent MS analysis.

Glycan analysis: Positive mode MALDI mass spectrometry was used to identify and semi-quantify released urothelial cell glycans following permethylation. MALDI spots were prepared using 2,5-dihydroxybenzoic acid solution (DHB, 10 mg/mL) that was mixed 1 : 1 (0.5 µL : 0.5 µL) with permethylated glycan samples in solution on the MALDI plate and the spot left to air dry. For semi-quantification experiments, the permethylated glycan samples containing *N*- and O-glycans were spiked with a solution of permethylated $GlcNAc_6$ (3 ng/µL) (1:1, v:v) as an

internal standard at the stage of forming the sample spot on the MALDI plate, semi-quantifying the amount of urothelial glycans.

Mass spectrometers: A solariX XR FT-ICR (Bruker Daltonics) equipped with a 9.4 Tesla magnet was the mass spectrometer mainly used for identification of permethylated glycans in this study. The mass spectrometer was calibrated externally using a standard peptide mixture. MALDI mass spectra were recorded over the *m/z* range 400-4000 with the acquisition of 12 scans, with each scan being collected by 500 laser shots. The laser power was adjusted between 30 and 50 %, to get a good response for permethylated glycans from a MALDI spot.

Potential *N*- and O-glycan structures were proposed by GlycoWorkbench [29] searched against peak lists generated from the MALDI FT-ICR mass spectrometric data, which provided mass accuracies typically of < 2 ppm for signals below *m/z* 2000. The GlycoWorkbench database is populated from the literature and so the structures it searches are published structures. For the list of candidate structures generated by GlycoWorkbench (searched using mass accuracy setting of < 40 ppm to allow all feasible structures to be included in the first pass results list), the accurate masses were then manually cross-checked against our experimental data, and only used if two or more isotopic signals were observed, to identify the correct composition. The proposed structures were then assessed against the relevant bladder glycoprotein literature, for example the lectin data and structures published by Yang et al [30].

Product ion analysis was conducted using the higher energy collision mode (HCD) using a Thermo Orbitrap Fusion Tribrid mass spectrometer (Thermo Scientific), in which the precursor ions were selected in the quadrupole and collided in the ion-routing multipole followed by mass

analysis in the Orbitrap. Permethylated glycan samples were dissolved in 80% methanol / 20% water / 0.1% formic acid and loaded into home-pulled emission tips to enable nano-electrospray ionisation. The MS/MS data were obtained with an isolation window set to 2 *m/z* and collision energy adjusted between 15-40%, depending on the *m/z* of the glycans and the signal abundance of precursors and fragments.

Quantification: Semi-quantification of each *N*-glycan species was carried out using the following method: 1) the peak intensities of the different isotopic signals with signal-to-noise ratio > 5 from the isotopic envelope of each *N*-glycan species were summed to generate a total signal intensity for each *N*-glycan species (denoted Σ_i); 2) the total peak intensities of all those *N*-glycan species common to all three biological replicates were summed for each spectrum (denoted Σ_T); and 3) this sum of peak intensities (Σ_T) was used to normalize the intensity of the signal for each *N*-glycan species (Σ_i) within the same MALDI mass spectrum. The normalized signal intensities for each *N*-glycan species from triplicate MALDI spots were averaged and the mean was used to derive the relative percentage of *N*-glycans in one technical replica.

RESULTS AND DISCUSSION

***N*- and O-glycan release from the apical urothelial surface**: To develop a method for urothelial apical glycan release we established tryptic-shaving approaches for releasing glycopeptides from the tissue surface. This involved exposing the urothelial surface of the opened bladder to trypsin solution, with the intent of liberating apical surface glycopeptides/peptides. Once isolated and recovered, these were subjected to PNGase F digestion and β elimination to release their *N*-and O- glycans respectively. For this approach to succeed, the superficial cell layer needed to retain its integrity under the conditions of trypsinization while demonstrating effective tryptic shaving of glycoproteins, to prevent compromising the preparation with glycopeptides/peptides from elsewhere in the tissue; to achieve this, two methodological development steps were introduced.

Step 1. Design of a device to maximise the surface area of the superficial urothelium available for digestion: A structural feature of the urinary bladder is that the empty bladder has numerous infoldings called rugae, which enable the bladder to expand as it fills with urine [31]. Preliminary investigations treating the opened, unextended bladder surface with trypsin showed inefficient glycopeptide release from the urothelium in regions protected by rugae. Because bladders are able to expand to accommodate filling with urine, it was anticipated that stretching the bladder to its natural accommodated state would not damage the tissue and would make the entire surface available for digestion.

A device was developed to enable bladder tissue to be held in a fully-extended state, thereby removing the urothelial zones protected by rugae. By being based on a conventional 6-well cell culture plate, the device further provides the advantage of six inbuilt reaction vessels for

replicate or serial testing on the same bladder lumenal surface (Figure 2A,, see also Supporting Information, and Figure S1, Figure S2). Porcine bladders were dissected and shaped by removing the top of the bladder above the ureters and the base to form a cylinder, and then cutting to open the bladder into a natural rectangle (Figure 2B, Figure S2). The rectangular shape aided in distributing the strain evenly across the tissue as it was stretched and held on the device (Figure 2A).

The bladder tissue examined using H&E staining showed histological structures, including the urothelium, remained fully intact after dissection (Figure 2C) and following accommodation (Figure 2D). The accommodated state was accompanied by a loss of rugae and by changes in collagen bundles in the bladder wall (stained pink by H&E) from compacted (Figure 2E) to aligned (Figure 2F), showing that the bladder was relaxed before stretching and completely distended on the reaction device.

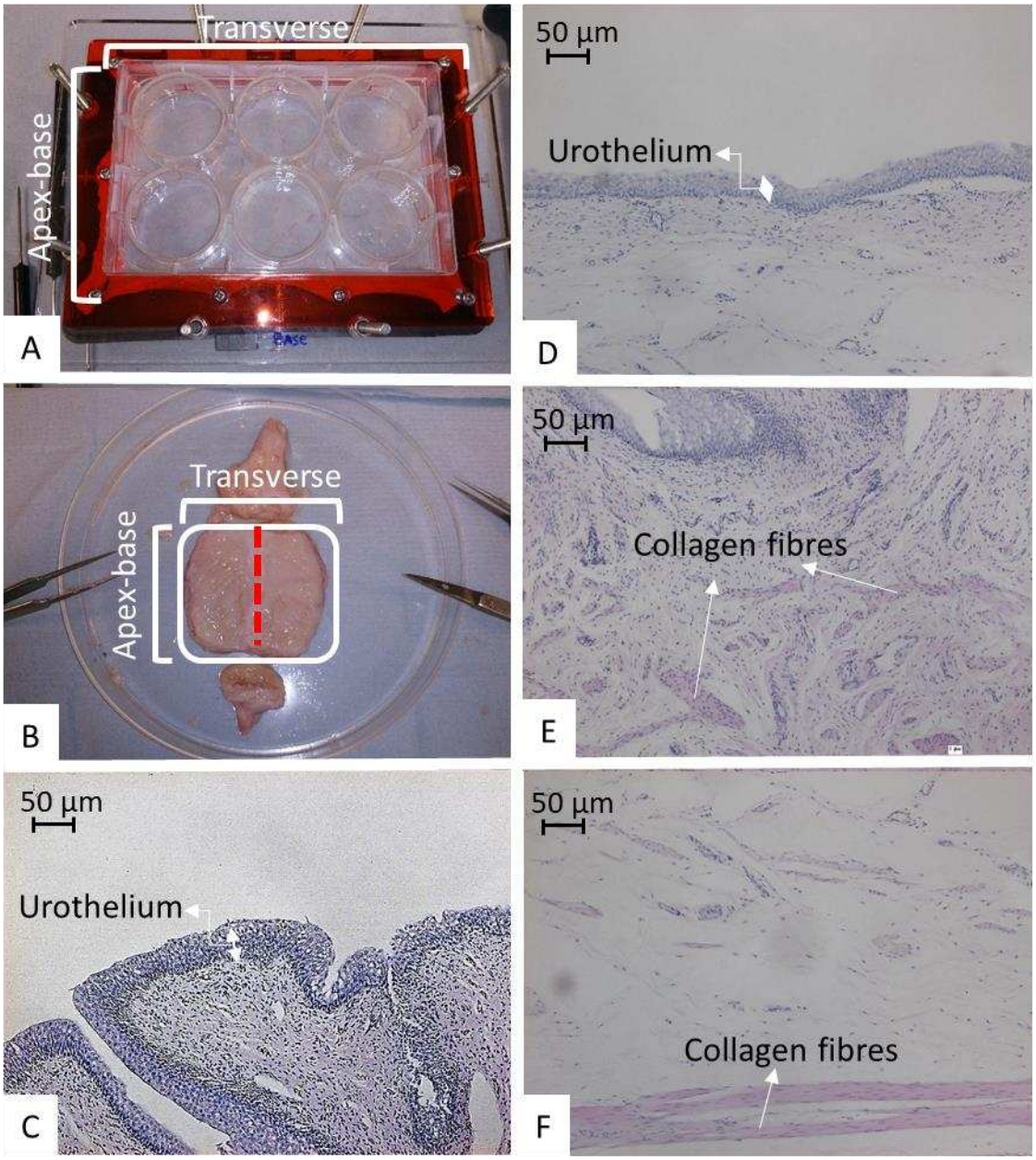

Figure 2. The reaction device providing 6 reaction chambers (A). A fresh pig bladder was dissected as shown in (B): after trimming to remove adventitious fat and connective tissue, the bladder was opened using scissors to remove the neck and apex before a longitudinal cut was made from neck to apex to open the bladder into a single-layered rectangular sheet, allowing the bladder tissue to lay in a low-stress flat sheet state. The dissected bladder was stretched on the reaction

device as shown in (A). The pig bladder before and after distending was processed for histology and examined using H&E staining. The urothelium remained intact before (C) and after (D) stretching, but with loss of anatomical folds or rugae. The collagen fibres (stained pink) in the relaxed bladder wall (E) showed realignment after stretching (F).

A leak test was conducted to ensure that the trypsin solution was retained within each vessel throughout trypsinization by weighing the trypsin solution before and after incubation. The mean recovery was 96.5% (1.90 ± 0.04 mg SD; n=4) which indicated the device sealed the trypsin solution with negligible exchange between adjacent vessels.

Monitoring tissue-surface trypsinization: In order to obtain objective evidence for the depletion of cell apical surface (glyco)proteins and inform optimization of the trypsin incubation time, UPK3a, an apically-expressed glycoprotein was examined post-digestion by immunohistochemistry using antibody AU1. UPK3a is a highly glycosylated apical surface protein and so an appropriate choice to identify conditions for effective digestion by trypsin (which can be hampered by glycosylation) while at the same time leaving the tissue surface intact. A complete urothelial surface layer was retained after the bladder was stretched (Figure 3A). Tissue sections collected from different bladder locations (in each of the six reaction wells) all gave identical immunolabelling results indicating an intact UPK3a layer across the urothelial apical surface before trypsinisation (Figure 3A).

Using individual wells in the reaction device made it possible to optimise tryptic digestion conditions. Different trypsin incubation periods (0, 2, 5, 10, 20, 40 minutes) were tested using individual wells, with immunolabelling of superficial UPK3a used to monitor the extent of loss

of the UPK3a layer from the apical surface with increased trypsin incubation (Figure 3B). UPK3a detected on the superficial porcine urothelium before trypsinization was still evident but reduced after 20 minutes' trypsinization and had depleted almost completely after 40 minutes' trypsinization (Figure 3B).

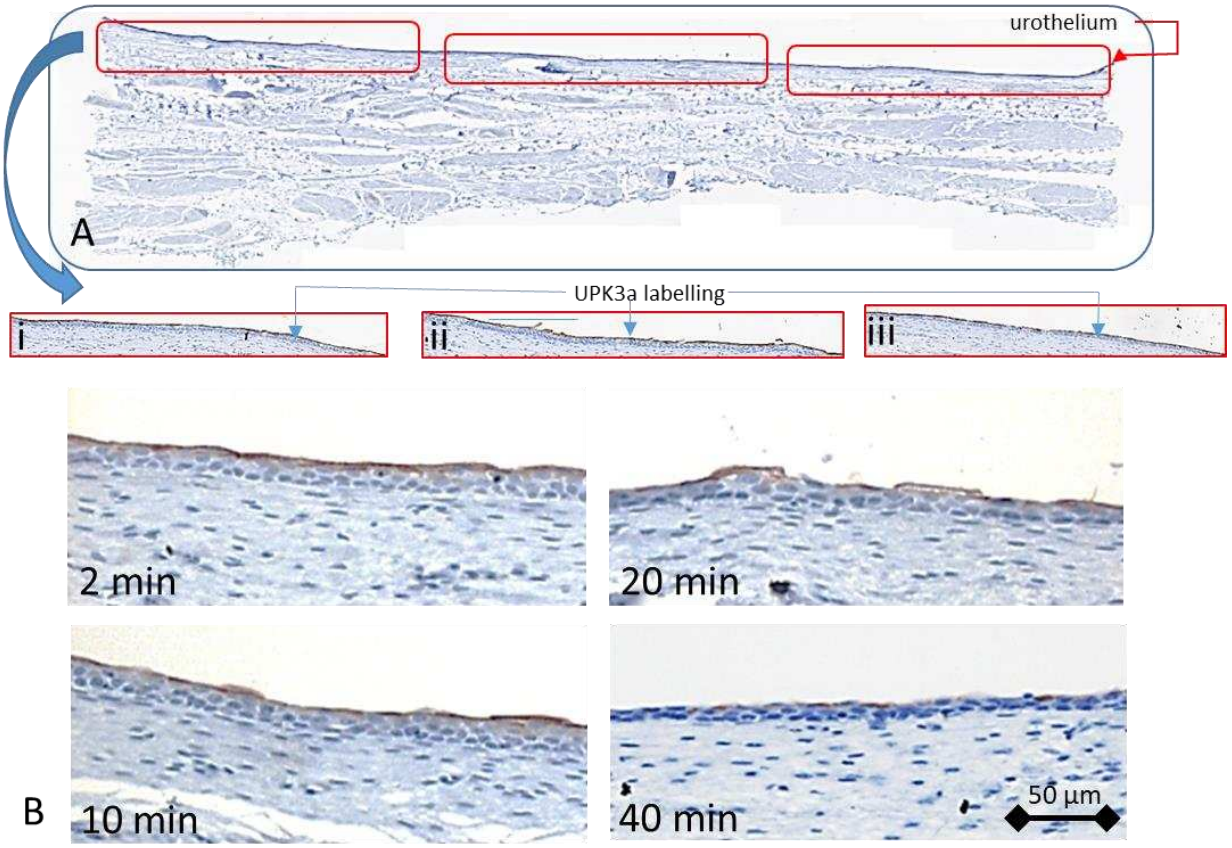

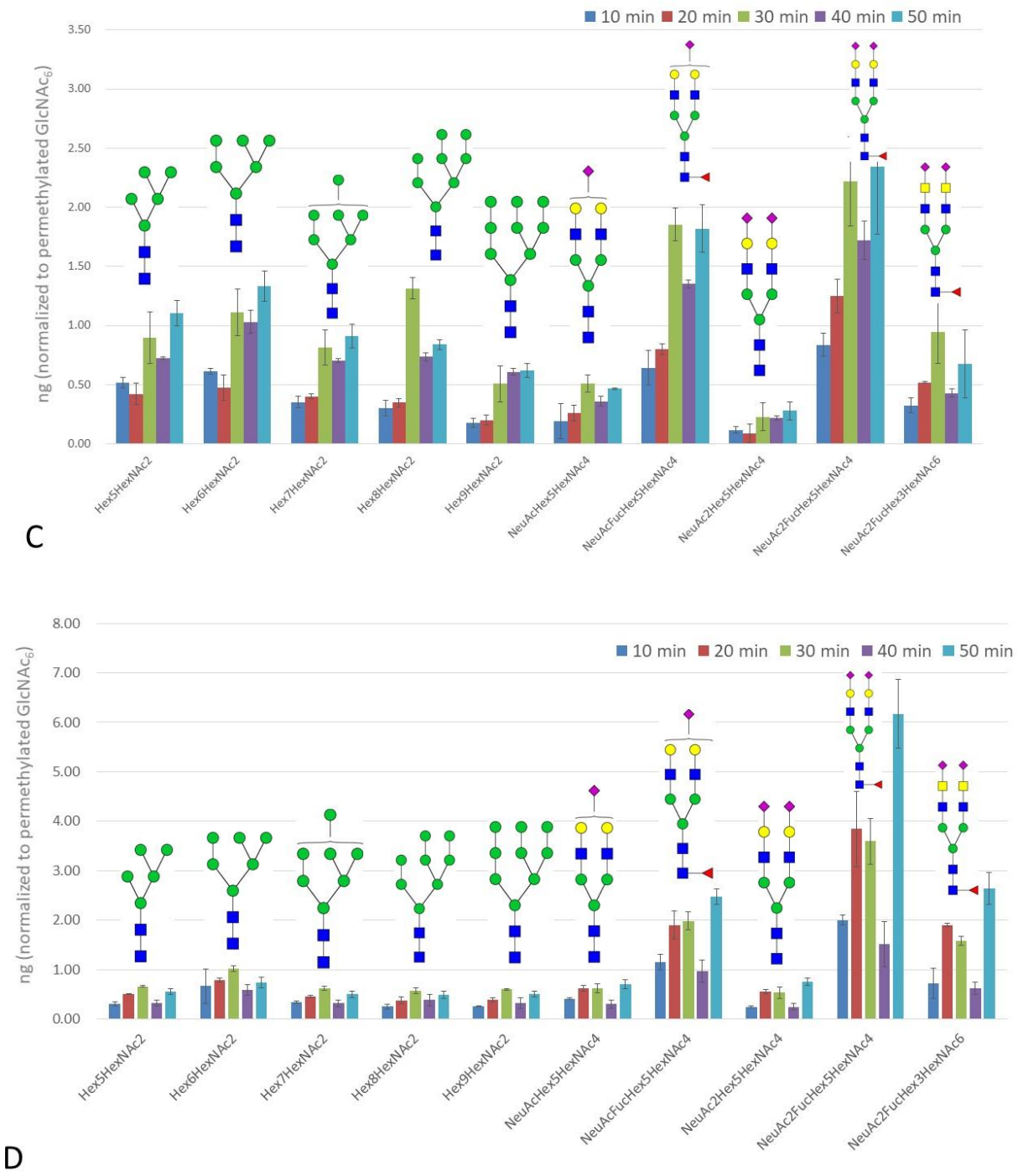

Figure 3. Monitoring of tissue-surface trypsinization. Stretched pig bladder was processed for (immuno)histology experiment to monitor the effects on tissue structure of tissue-surface trypsinization (panels A, B), while MALDI-MS assessed the outcome of the tryptic shaving

optimization for *N*-glycan release study (panels C, D). (A) Histological section through porcine bladder indicating position of reaction vessels labelled in replicate for UPK3A (a, b & c) to show reproducibility. (B) Immunolabelling of porcine urothelium labelled with UPK3A following surface trypsinisation for 2, 10, 20 and 40 minutes. Note the reduction of labelling over time. These results were ranked by seven independent (blinded) observers and the linearity between the average ranking score for each slide and the period of trypsinization was tested by linear regression ($P \geq 0.0005$), supporting the relationship between immunolabelling for UPK3a and extent of trypsinization. The amount of each *N*-glycan species (potential structures are depicted) released from the luminal surface of porcine bladders 1 (C) and 2 (D), using on-tissue trypsinization for 10, 20, 30, 40 or 50 minutes. Error bars indicate the standard deviations of the mean for three technical replicates.

Optimisation of surface shaving time and *N*-glycan release for MALDI-MS: Optimised tryptic digestion of urothelium was carried out in Hank's balanced salt solution (HBSS) which, although not ideal for use with samples for mass spectrometric analysis (it contains, among other things, calcium and magnesium salts), was demonstrated to be necessary to maintain the tissue surface intact (not shown). To overcome this conflict a scheme for cell surface glycan release and analysis was developed to purify glycan mixtures obtained from the sample matrix containing inorganic salts (Figure 4).

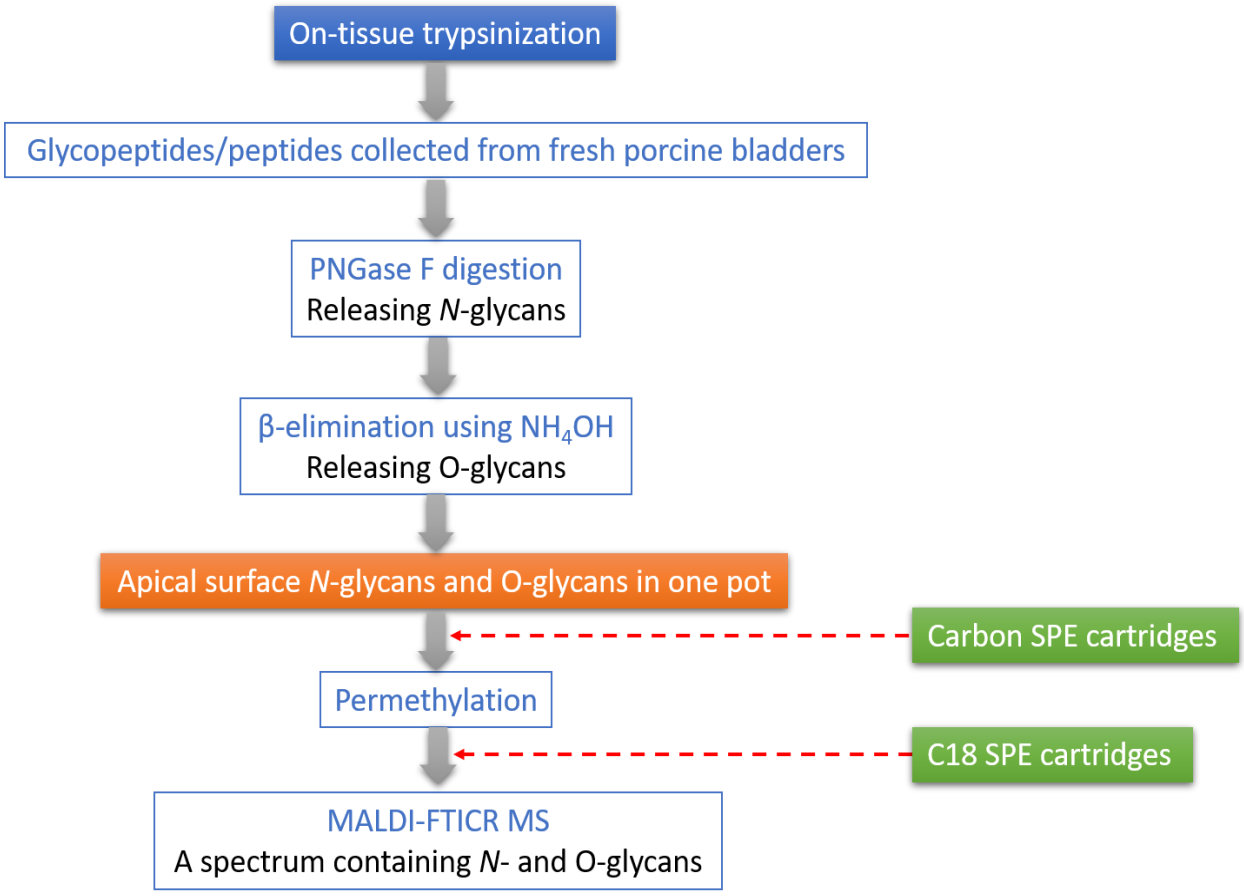

Figure 4. Scheme for cell surface glycan release and analysis, developed to purify glycan mixtures obtained from the sample matrix containing inorganic salts. Collected trypsinized supernatants were subjected to PNGase F digestion and β-elimination to release *N*- and O-glycans that were isolated as a single pool using graphitized carbon SPE (e.g. 25) to purify the glycans from the HBSS salts, and then permethylated and purified using C18 SPE (e.g. 19,25). Permethylated glycan samples containing *N*- and O-glycans were spiked with permethylated $GlcNAc_6$ as an internal standard at the stage of forming the sample spot on the MALDI plate, for analysis using MALDI-MS, semi-quantifying the amount of urothelial glycans.

The amounts of *N*-glycans released from the luminal surface of two porcine bladders accommodated onto the stretching device and incubated with trypsin for different time periods were analyzed following permethylation and quantification with an internal standard (permethylated $GlcNAc_6$) using MALDI-MS. Ten different *N*-glycans were identified in the two minute incubation sample and were common to the other samples incubated for longer, their levels increasing with increased incubation time (Figure 3C, D). The amount of each *N*-glycan species released from the two bladders increased only slowly after 30 minute trypsin treatment and extending the length of trypsinization did not release more different *N*-glycan species (Figure 3C, D). Consequently, a 30-minute trypsin incubation period was adopted for all future experiments.

Porcine urothelial cell apical surface *N*- and O-glycans: Having established that the tryptic treatment of tissues in the 6-well device specifically and efficiently releases apical surface components from accommodated porcine bladders, the approach was used to release the apical surface glycopeptides from three replicate porcine bladders collected on the same day and processed in parallel. *N*- and O- glycans were retrieved in a single pool from the trypsin supernatants on sequential PNGase F and subsequent alkaline β-elimination [32] treatments, respectively. The uroglycome was isolated using graphitised carbon solid phase extraction [19, 33] which proved to be an efficient way to purify the glycans from the HBSS salts in which the tissue was enzymatically shaved, and then permethylated and purified using C18 solid phase extraction [19, 27, 33], for MALDI mass spectrometric semi-quantitative analysis (carried out as in (22)). Importantly, it was not possible to obtain mass spectrometric signals from the permethylated released glycans without isolating them before permethylation using graphitised carbon SPE, presumably due to the very complex matrix presented by the HBSS buffer. Use of

C18 SPE to purify glycans after permethylation enhanced signal:noise, signal stability and mass spectrometric response, even when glycans had been isolated using graphitised carbon SPE, and so this step was routinely incorporated in our protocol.

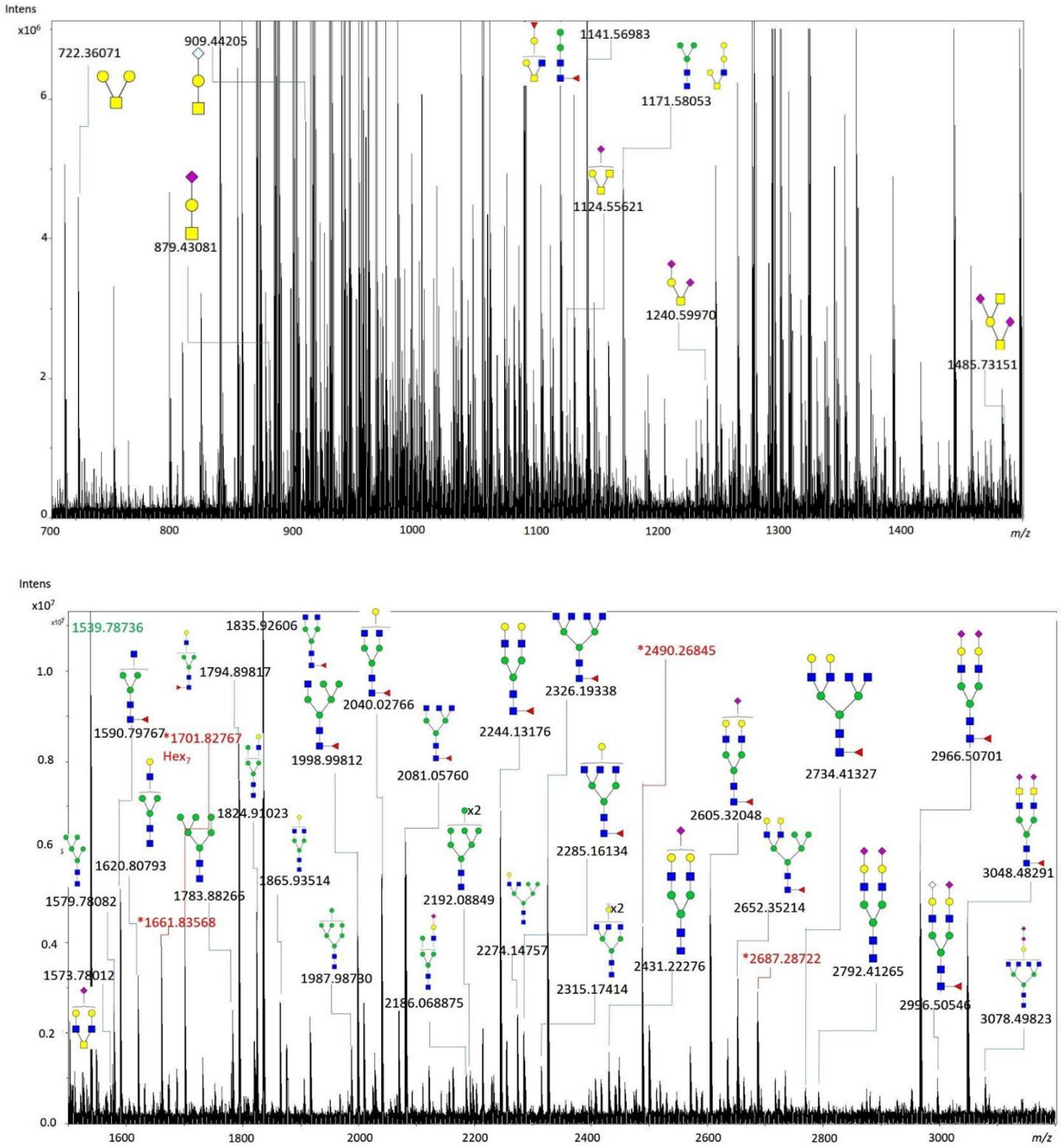

Figure 5. Representative MALDI mass spectrum of porcine urothelial cell apical surface *N*-glycan and O-glycan profiles obtained from the luminal surface of porcine bladder, upper panel displays *m/z* 700 to 1500 (the proposed *N*- and O-glycan structures of peaks ($M+Na^+$) are depicted). Lower panel displays *m/z* 1500 to 3200 (the proposed structures of intense peaks ($M+Na^+$) are depicted). Asterisks represent intense signals not readily assignable as O- or *N*-glycans. The different intensity axes on the two panels have been used to display the glycan signals most conveniently, and to enable them to be observed against the high background that is due to contaminating Glc oligomers in the HBSS buffer, that are incompletely removed during the sample-handling procedure.

Representative MALDI mass spectra obtained from the *N*- and O-glycans from the three individual porcine bladders after permethylation were very similar to each other, the main difference between the spectra being their relative peak intensities. A typical MALDI mass spectrum is shown (Figure 5). Most of the peaks for apical cell surface *N*-glycans were much more intense than those for apical cell surface O-glycans. For apical cell surface O-glycans, intense peaks were assigned as mucin-type O-glycans at *m/z* 722.36 ($Hex_2HexNAc$), 879.43 (NeuAcHexHexNAc), 909.44 (NeuGcHexHexNAc), 1124.56 ($NeuAcHexHexNAc_2$), 1240.60 ($NeuAc_2HexHexNAc$) and 1485.73 ($NeuAc_2HexHexNAc_2$). For apical cell surface *N*-glycans, the most intense peaks in all the mass spectra can be assigned to complex *N*-glycans at *m/z* 1794.90 ($FucHex_4HexNAc_3$), 1835.92 ($FucHex_3HexNAc_4$), 2040.03 ($FucHex_4HexNAc_4$), 2081.06 ($FucHex_3HexNAc_5$), 2244.13 ($FucHex_5HexNAc_4$), 2326.19 ($FucHex_3HexNAc_6$), 2605.32 ($NeuAcFucHex_5HexNAc_4$), 2652.35 ($FucHex_7HexNAc_4$), 2966.51 ($NeuAc_2FucHex_5HexNAc_4$), and 3048.48 ($NeuAc_2FucHex_3HexNAc_6$). It should be noted that

the peaks at *m/z* 1141.57 ($FucHex_2HexNAc_2$) and 1171.58 ($Hex_3HexNAc_2$) can be assigned as either *N*-glycans or O-glycans; see discussion below of Figures S8 and S9.

In total, 55 different urothelial cell apical surface *N*-glycans (Supporting Information Figure S3) and 12 different O-glycans (Supporting Information Figure S4) were identified over the three biological replicates. Small standard deviations in relative signal intensities (shown on Figures S1 and S2 and provided, with CVs, in Tables S2 and S4) were obtained among experimental replicates for most of the *N*- and O-glycan species, demonstrating that the developed protocol (Figure 1) for on-tissue trypsinization followed by sequential glycan release using PNGase F digestion and β-elimination, is capable of giving high reproducibility of data for apical cell surface glycan identification. Most porcine urothelial cell apical surface glycan structures were identified across all three biological replicates (Supporting Information Figure S5); 47 of the 55 *N*-glycans (Supporting Information Figure S6) were identified in all three biological replicates (Supporting Information Table S1), and all 12 apical cell surface O-glycan structures (Supporting Information Figure S7) were identified in all three biological replicates (Supporting Information Table S3).

The results generated using this approach represent the first normal mammalian superficial urothelial cell apical surface *N*- and O-glycome. The apical cell surface *N*- and O-glycomes obtained using the on-tissue trypsinization approach showed great reproducibility between biological replicates in both the relative amount of released glycan (based on the small standard deviations) and the number of different glycan species detected (Supporting Information Figure S5). A few apical cell surface *N*- and O-glycans differed in terms of their proportion of the total common glycans between biological replicates, likely due to individual biological variation. It should be noted that information on the breed, age, and sex of the animals from which the

bladders derived was not available from the abattoir. Such background information may help to explain individual differences observed in glycan profiles in future studies.

In order to verify the structural assignments proposed on the basis of composition, knowledge of biosynthesis, the specific literature, and well established *N*- and O-glycan structures, product ion analyses were conducted to investigate some representative apical cell surface glycans, released together in a mixture from porcine urothelium. The candidate glycans for product ion analysis included 1) two groups of potentially *N*- and O-glycans identified at *m/z* 1141.57 (Supporting Information Figure S8) and 1171.58 (Supporting Information Figure S9), 2) basic oligomannose *N*-glycan at *m/z* 1579.69 (Supporting Information Figure S10), 3) basic hybrid *N*-glycan at *m/z* 1824.91 (Supporting Information Figure S11) and 4) basic complex *N*-glycan at *m/z* 1835.93 (Supporting Information Figure S12). Product ion analysis was conducted using the higher energy collision mode (HCD) on a Thermo Orbitrap Fusion Tribrid.

In summary, the product ion spectrum of $FucHex_2HexNAc_2$ at *m/z* 1141.57 (Supporting Information Figure S8) suggests a single linear *N*-glycan species; no fragment ions were consistent with the presence of a typical isobaric O-glycan. The product ion spectrum of $Hex_3HexNAc_2$ at *m/z* 1171.58 (Supporting Information Figure S9) shows two sets of fragments in a chimeric spectrum, which can derive from the *N*- and O-glycan isomeric forms of $Hex_3HexNAc_2$. The product ion spectrum of $Hex_5HexNAc_2$ at *m/z* 1579.67 (Supporting Information Figure S10) is consistent with the expected Hex_5 oligomannose glycan structure. The product ion spectra of *m/z* 1824.91 ($Hex_5HexNAc_3$, Supporting Information Figure S11) and 1835.93 ($FucHex_3HexNAc_4$, Supporting Information Figure S12) both show two sets of fragments consistent with the presence of two isomeric hybrid *N*-glycan isomers.

Step 2. Collection and analysis of *N*-glycans from whole urothelium isolated from bladder tissue: For comparison with the apical uroglycome, the whole epithelial glycome was investigated by analyzing *N*-glycans released from porcine urothelium which was harvested by scraping the luminal surface of the bladder with a scalpel to release the urothelium from the tougher underlying stromal tissue at the natural junction of the collagen IV-rich basement membrane, which was monitored by immunohistochemistry (Supporting Information Figure S13).

Three different fresh porcine bladders (Uro1, Uro2 and Uro3) were used as the source of normal porcine urothelial cells, representing three biological replicates from which whole porcine urothelial cell *N*-glycan profiles were obtained. For technical replicates, three aliquots of urothelial cells from each of the three bladders were used side by side for *N*-glycan release using whole cell lysis and the FANGS protocol [23]. Representative MALDI mass spectra obtained from three individual porcine bladders revealed 46 different urothelial *N*-glycans taking the three biological replicates together; the proposed structures for the glycans represented by the most intense peaks are depicted in Supporting Information Figure S14. The most intense peaks in all the mass spectra of porcine urothelial *N*-glycans can be assigned as oligomannose *N*-glycans at *m/z* 1579.79 ($Hex_5HexNAc_2$), 1783.89 ($Hex_6HexNAc_2$), 1987.99 ($Hex_7HexNAc_2$), 2192.09 ($Hex_8HexNAc_2$) and 2396.20 ($Hex_9HexNAc_2$). Mono- and di-sialylated complex *N*-glycans were observed above *m/z* 2000, including *m/z* 2431.21 ($NeuAcHex_5HexNAc_4$), 2605.30 ($NeuAcFucHex_5HexNAc_4$), 2635.31 ($NeuGcFucHex_5HexNAc_4$), 2966.45 ($NeuAc_2FucHex_5HexNAc_4$) and 2996.45 ($NeuAcNeuGcFucHex_5HexNAc_4$). The relative

percentages of those porcine urothelial total cell lysate *N*-glycans common to all three biological replicates are shown in Supporting Information Figure S15.

The most abundant *N*-glycan classes in each biological replica were the complex *N*-glycans that represented 55.0%, 61.6% and 56.9% of the common *N*-glycome in the three biological replicates, respectively,while the respective proportion of oligomannose *N*-glycans was 37.7%, 30.0% and 38.3%. The proportion of hybrid *N*-glycans was less than 5% in all samples. The ~3-5 % of *N*-glycan structures smaller than $Hex_2HexNAc_5$ were presumed to be degraded *N*-glycans and not categorized into any group. Small standard deviations in relative signal intensities (n=3) were obtained among technical replicates for each *N*-glycan structure, consistent with the FANGS approach being capable of giving highly reproducible MALDI mass spectra, which is in line with the results of the studies by Abdul Rahman et al. [23] and Skeene et al. [24].

Most *N*-glycan structures were identified at similar proportions in all three biological replicates (Supporting information Figure S16). Of these 46 *N*-glycans, 29 were present in all biological replicates (Supporting Information Table S5, Supporting Information Figure S15). The 17 *N*-glycans identified in one or two biological replicates represented generally less than 1% of the averaged total intensities of all *N*-glycans in each biological replicate and had low absolute signal intensities (<106 counts), and so represent a very small proportion of the total urothelial *N*-glycans in the total cell lysate *N*-glycans.

One particular monosialylated monoantennary *N*-glycan identified in the three biological replicates, $NeuAcHex_3HexNAc_3$ was not reported in previous urothelial *N*-glycan studies [24] but was identified on human neutrophil cathepsin G (nCG) [34] and human bone marrow-derived mesenchymal stem cells (MSC) [35] using LC-MS/MS and MALDI-MS of underivatized glycan

preparations, respectively. Sample Uro2 data contained particularly low percentages of $Hex_5HexNAc_2$ and $NeuAc_2FucHex_5HexNAc_4$ and had more different complex *N*-glycan species ($FucHex_5HexNAc_3$, $NeuGcHex_4HexNAc_3$, $Fuc_2Hex_4HexNAc_4$, $Hex_6HexNAc_4$, $FucHex_3HexNAc_6$, NeuAcFuc $Hex_5HexNAc_4$, $NeuAcHex_5HexNAc_4$, $NeuGcFucHex_5HexNAc_4$ and $NeuAcFucHex_6HexNAc_5$) than Uro1 and Uro3. Since the three porcine bladders were collected and processed at the same time, this difference is likely to be caused by individual biological differences and not by variation in sample handling, since there is a small standard deviation across the technical triplicates.

DISCUSSION

Here, we present a novel validated approach that defines the polarised urothelial tissue surface glycome. We have used it to generate the first description of a normal apical tissue surface glycome, and so are in a position, for the first time, to consider the purpose of the glycans in urothelial biology. Whilst obtaining human bladder tissue in sufficient quantities to carry out such experiments on normal human urothelium may be challenging, our approach could in future be applied to in vitro-generated barrier-forming human urothelium [36], enabling us in further studies to determine the effect on the surface glycome of treating the bladder lumen with drugs or devices. Given the widespread but not un-controversial use of intravesicular glycosaminoglycan therapies [14, 37-41], our approach may also open opportunities for evidence-based investigations of the effects of such glycome therapies. It is worth noting that our method could be expanded to include the study of GAGs, if these did indeed prove to be relevant to the bladder urothelial barrier function. While our method was designed to examine the bladder glycome, our approach could be adapted (including identifying surface markers to monitor digestion) and optimized for application to other epithelial surfaces lining tracts and organs,

including skin and different regions of respiratory, alimentary and reproductive tracts. It could also be used to study other surface tissues such as cartilage.

Comparison of the apical surface glycome with the whole urothelial tissue glycome (see Figure 6 and its discussion, below) has enabled identification of glycans found only in the apical surface preparations. With the identification here for the first time of apical-specific glycan structures, there is now the prospect in future studies of ascribing functional roles to these surface glycans.

The comparison between the urothelial total cell lysate *N*-glycome and the urothelial apical surface *N*-glycome revealed distinct differences in the number and proportions of *N*-glycan species identified. This observation is in line with the results of studies by other research groups where the identification of cell surface *N*-glycomes released either from enriched cell membrane fractions [2, 3, 42] or from cell surface tryptic shavings [1] were compared to total cell lysate *N*-glycomes. In addition, the high proportion of urothelial complex *N*-glycans released from either the total cell lysate or on apical cell surface shaving may present a signature of highly specialised cells. This is supported by the results of the study by Montacir and colleagues [19] in which the authors used cell surface trypsinization to collect the cell surface *N*-glycans from cultured human embryonic stem cells (hESCs) and cultured hepatocyte-like cells (HLCs), directly differentiated from the hESCs. Montacir et al. classified the complex *N*-glycans into several groups with sialylation or fucosylation and only reported the number of biantennary and oligomannose. The proportion of biantennary complex *N*-glycans released from the hESC-differentiated HLCs increased to 49% from 11% in the hESCs. By contrast, the proportion of oligomannose *N*-glycans released from the hESC-differentiated HLCs reduced to 18% from 39%.

Prior to the present study, there is only a single report [24] of urothelial O-glycan structural studies that we are aware of, and most reports of urothelial *N*-glycans relate to the species-dependent uroplakin *N*-glycoforms [6, 7, 9, 10, 43-45]. A summary of those urothelial *N*-glycan structures identified in previous studies includes oligomannose ($Hex_{5-9}HexNAc_2$), hybrid, and bi, tri-, and tetra-antennary complex glycans bearing one to four fucose and sialic acid residues in bovine and mouse uroplakins [6, 10, 24, 30, 43, 46, 47]. Human urothelial *N*-glycans have been reported to contain the structures listed above, as well as a proposed intersecting GlcNAc glycoform [30].

The recent study of Skeene et al. [24] used lysates of whole porcine urothelial cells prepared by scraping, as in this study, to develop a one-pot method using FANGS to sequentially release *N*- and O-glycans from urothelial cell lysates; that study reported 16 *N*-glycans containing five oligomannose *N*-glycans ($Hex_{5-9}HexNAc_2$), six complex *N*-glycans ($Hex_3HexNAc_4$, $FucHex_3HexNAc_4$, $Hex_4HexNAc_4$, $NeuAcFucHex_5HexNAc_4$, $NeuAc_2Hex_5HexNAc_4$, $NeuAc_2FucHex_5HexNAc_4$) and others ($Hex_2HexNAc_2$, $FucHex_2HexNAc_2$, $Hex_3HexNAc_2$, $FucHex_4HexNAc_2$, $Hex_4HexNAc_2$). All 16 *N*-glycans identified in that study were also identified in the urothelial whole cell lysates reported here. High abundance of oligomannose *N*-glycans and a relatively low abundance of complex *N*-glycans were reported by Skeene et al [24]. By contrast, in the present study, along with the detection of the same oligomannose *N*-glycans, many complex *N*-glycans were identified that were at low abundance or not detected by Skeene et al. It is not clear what caused the difference in the relative abundances of total cell lysate *N*-glycans between the two different studies using the same method, and similarly prepared urothelial cells from the same species. A likely explanation is that the amount of urothelial cells used to release the total cell lysate *N*-glycans in this study could have been higher (approximately $2 \sim 3 \times 10^6$ cells) than the amount of urothelial cells used in the study by Skeene

et al. (where the amount was not reported), enhancing the detection of many low abundance complex *N*-glycans in the high *m/z* range.

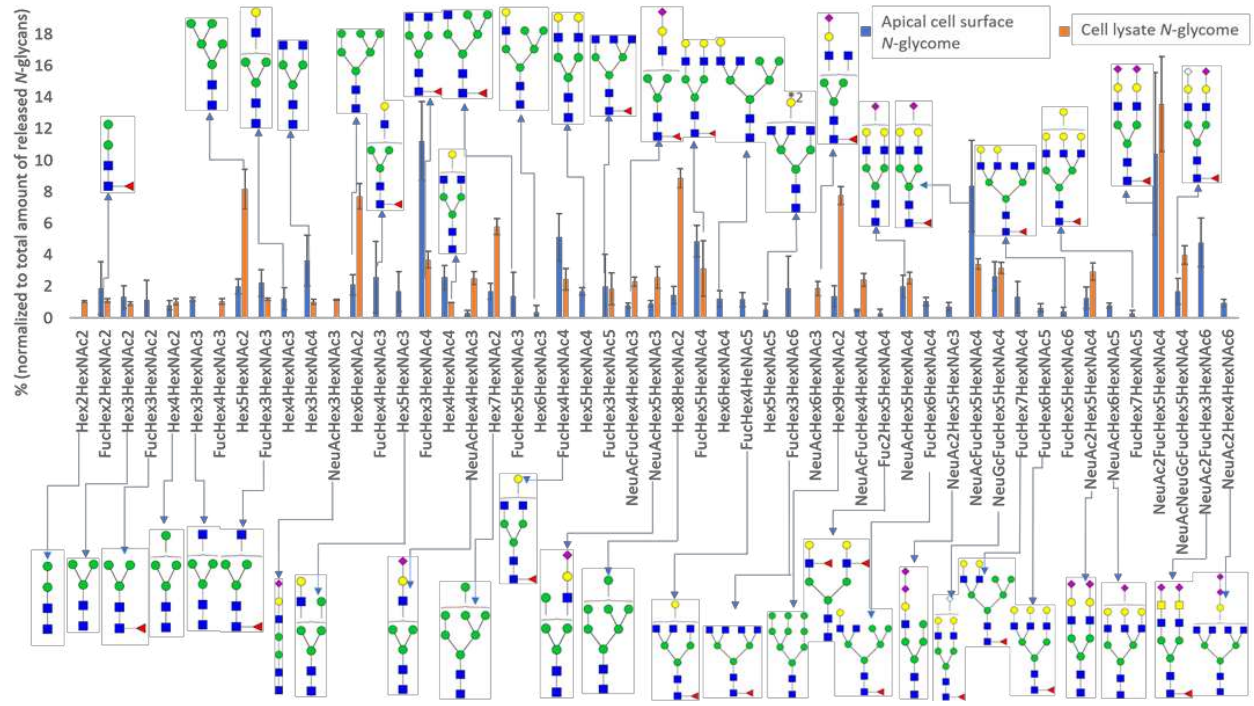

A

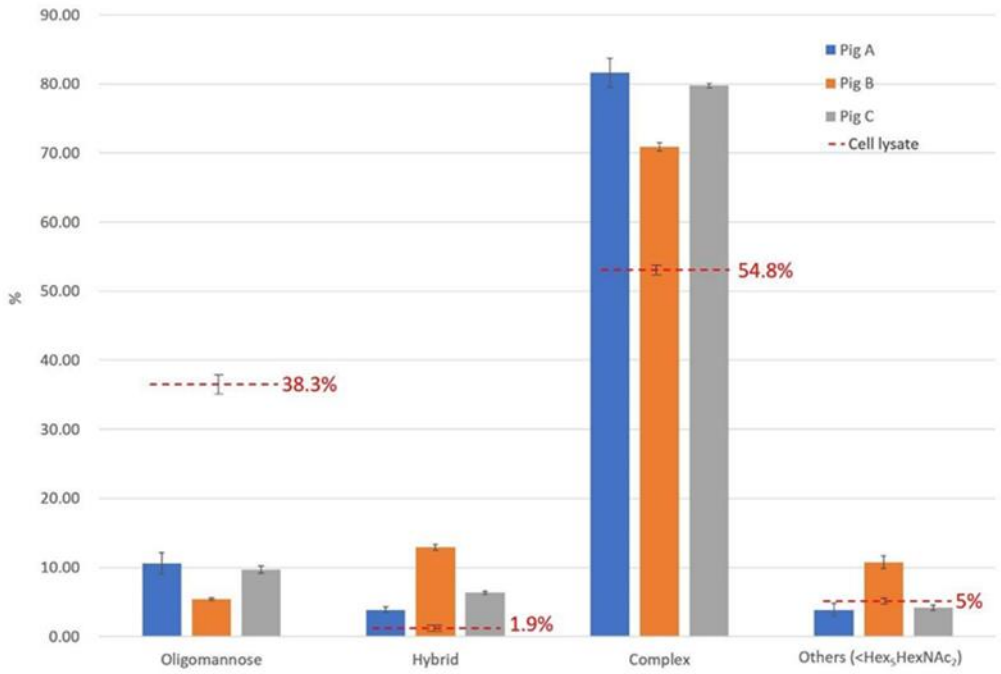

B

Figure 6 A. The relative percentages of porcine urothelial total cell lysate *N*-glycan proposed structures compared to those of porcine urothelial cell apical surface structures. B. The percentages of oligomannose, hybrid, complex and other *N*-glycans in the porcine urothelial cell apical surface *N*-glycome of three biological replicates using the on-tissue trypsinization approach. The red dotted lines indicate the percentages of the different types of *N*-glycan, representing the means of the three biological replicates, in the porcine urothelial total cell lysate *N*-glycome.

The relative percentages of the 47 *N*-glycans in the porcine urothelial cell apical surface *N*-glycome released using on-tissue trypsinization (Figure 6A) were compared with the relative percentages of the 29 *N*-glycans in the porcine urothelial total cell lysate *N*-glycome identified using the FANGS approach. It is noteworthy that 22 *N*-glycan structures were identified only in the apical cell surface *N*-glycome, of which 20 were complex and hybrid *N*-glycans, and two were smaller than $Hex_5HexNAc_2$. By contrast, four *N*-glycan structures were identified only in the total cell lysate *N*-glycome, of which two were complex *N*-glycans and two were smaller than $Hex_5HexNAc_2$. The apical surface *N*-glycan structures can be divided into four structural groups (Figure 6B). The proportion of complex *N*-glycans released from the porcine urothelial cell apical surface increased to 77.5% from 54.8% from total cell lysates. By contrast, the proportion of oligomannose *N*-glycans released from the apical cell surface reduced to 8.6% from 38.3% in the total cell lysates. In addition, 20 more complex *N*-glycans were identified only in the apical cell surface *N*-glycome.

To date, biological functions of glycans on urothelium have not been studied, with the sole exception of the demonstration of the function of the oligomannose glycans of UPK1a [10, 11, 48]. Urothelial *N*-glycans have been mainly investigated in studies of *N*-glycosylation of uroplakins, or in cell lysate glycomes from established bladder cancer cell lines. In the present study, providing the first normal mammalian urothelial *N*-glycome, low abundance oligomannose *N*-glycans and high abundance complex *N*-glycans were observed in both apical cell surface *N*-glycomes and the total cell lysate *N*-glycome of scraped porcine urothelium. The high abundance of complex *N*-glycans observed here in urothelium, and suggested by Montacir et al [19] (in hESCs) to be a feature of differentiation, raises intriguing prospects for polarised epithelial surface biology. Urothelial O-glycans have been mainly identified as mucin-type structures in

previous studies, using lectin labelling of O-glycans in animal tissues or cell lysates [13, 49-51]. Some studies have suggested that the urothelium is a type of secretory epithelium, because most glycan structures labelled by lectins were mucin-type O-glycans (T and Tn antigens) that are commonly identified in mucus secreted at mucosal epithelial surfaces [49, 51]. However, urothelium is not classified as a mucosal epithelium [52]. Based on the observation that the O-glycans identified in the present study required trypsinization to shave the apical cell surface prior to β-elimination to release O-glycans, it is proposed that the inferred urothelial mucin-type O-glycans are unlikely to be from secreted proteins but from the membrane-bound glycoproteins present on superficial urothelium. A control on-tissue treatment was conducted in the present study using buffer without trypsin; no detectable mass spectrometric signals for O- and *N*-glycans were obtained on MALDI-MS. This result suggests that the porcine urothelium does not have secreted glycoproteins and is unlikely to be a secretory epithelium, which is in line with the results of N'Dow et al. [52] in which the quantities of bladder surface-associated glycoproteins were shown to remain constant, although the amounts of urinary glycoprotein were very variable; this perhaps indicates derivation from elsewhere in the urinary tract.

It is possible that there are parallels between the apical surface glycan structures we report here, and the role of *N*- and O-glycan structures that have been associated with apical targeting in other polarised epithelial cells. In one such study, fucosylation of *N*-glycans was described as a signal for apical targeting of biliary glycoproteins [53]. In a study by Kinlough et al., the O-glycans on MUC1 were demonstrated to be the signal required for sorting to the apical surface of polarised MDCK cells [54]. Specifically, the latter study demonstrated that overexpression of α2,6-sialyltransferase-1 resulted in depletion of core 1 mucin-type O-glycans and the relocalisation of MUC1 to the basolateral rather than apical surface of MDCK cells. Our observations of

fucosylated *N*-glycans and mucin-type O-glycans on the urothelial apical surface of the urothelium are thus consistent with a role for such glycans in defining the polarised apical surface of differentiated epithelial cells and tissues.

To summarise, total cell lysate urothelial *N*-glycans and apical cell surface *N*- and O-glycans from the luminal surface of fresh polarized porcine superficial urothelium have been successfully investigated using FANGS and on-tissue trypsinization, respectively. The use of an in-house built device with six reaction wells enabled tissue-surface trypsinization and allowed multiple experimental replicates of the uniform luminal surface of stretched porcine bladders to be studied for the first time. The value of separating (apical) surface glycans from total cell lysate glycans is to offer a glycan profile of the polarized cell surface to explore those glycans that are potentially responsible for various tissue apical surface features. Moreover, this six-well device also allowed post-processing of porcine bladder samples by formalin fixation immediately after trypsinization, chemically preserving the appearance of the trypsinized cell surface for immunohistochemical monitoring and validation of the extent of trypsinisation. This has made it possible to visualize the site of shaving of the tissue and to demonstrate that the tissue handling treatments did not compromise the tissues and thus the samples produced. It enables the specific study of the apical cell surface glycome from fresh animal tissues, presenting a method to examine, in real time, the expression of glycans/peptides/proteins on differentiated tissue surfaces with structural information generated by MS analysis. It should be noted that our shaving approach yields glycopeptides. These glycopeptides can be processed and analysed using the full range of different glycopeptide and glycan analysis approaches available (for reviews of such analytical approaches, see [55-57]), and so our method is flexible for

implementation with other analytical approaches beyond those we used here to release and profile the apical *N*- and O-glycomes.

This study represents the first study of a mammalian uroglycome. The porcine bladder urothelium is anticipated from other studies to be similar to that of human bladder. Consequently, porcine urothelial glycan profiles can be considered a preview of human urothelial glycan profiles, with a processing pipeline available for subsequent studies using barrier-forming in vitro propagated and differentiated human urothelial cells in lieu of hard-to-source primary human bladder tissue. The transition to an in vitro approach will also enable molecular tools to be incorporated to study glycan functions – for example by following the approach of Kinlough [54] by overexpressing CMP-Neu5Ac:GalNAc-R2,6-sialyltransferase-1 to block core O-glycan synthesis and assess the impact on barrier function and surface protein expression.

Our two approaches have been demonstrated to be capable of determining qualitative and semi-quantitative urothelial glycan profiles, enabling comparative studies that will allow determination of the potential functional contributions of individual glycans to urothelial function, development of urothelial diseases, and study of the mechanisms of action on the urothelial glycome of treatments and devices.

ASSOCIATED CONTENT

The following files are available free of charge:

SUPPORTING INFORMATION:

The following supporting information is available free of charge at ACS website http://pubs.acs.org

Device for on-tissue trypsinization for release of apical cell surface glycopeptides. Text describing the device for on-tissue sampling and how it is used.

Figure S1. Schematic depicting design and use of device for on-tissue trypsinisation

Figure S2. Photographs showing dissection of porcine bladder and stretching onto device base plate.

Figure S3. The collection of 55 porcine urothelial cell apical *N*-glycans from three biological replicates (semi-quantification of proposed *N*-glycans from the apical surface of three different pig bladders)

Figure S4. The collection of 12 permethylated porcine urothelial cell apical O-glycans from three biological replicates (semi-quantification of proposed O-glycans from the apical surface of three different pig bladders)

Figure S5. Venn diagram showing the distribution of the 55 different porcine urothelial cell apical surface *N*-glycans over the three biological replicates

Figure S6. Relative percentages of the 47 porcine urothelial cell apical surface *N*-glycans that were common to the three biological replicates (relative amounts of the 47 common *N*-glycans observed in the apical glycome of three replicate pig bladders)

Figure S7. Relative percentages of the 12 porcine urothelial cell apical surface O-glycans that were common to the three biological replicates (relative amounts of the 12 common O-glycans observed in the apical glycome of three replicate pig bladders)

Figure S8. Product ion spectrum of $[M+Na]^+$ at *m/z* 1141.57, in permethylated glycans collected from porcine urothelium using on-tissue trypsinization (MSMS data demonstrate a linear structure consistent with a truncated *N*-glycan, rather than a branched O-glycan isomer)

Figure S9. Product ion spectrum of $[M+Na]^+$ at *m/z* 1171.58, in permethylated glycans collected from porcine urothelium using on-tissue trypsinization (MSMS data allow the presence of both *N*- and O-glycan isomers of $Hex_3HexNAc_2$ to be identified)

Figure S10. Product ion spectrum of $[M+Na]^+$ at *m/z* 1579.79, in permethylated glycans collected from porcine urothelium using on-tissue trypsinization (MSMS data are consistent with a standard $Man_5GlcNAc_2$ oligomannose glycan)

Figure S11. Product ion spectrum of $[M+Na]^+$ at *m/z* 1824.91, in permethylated glycans collected from porcine urothelium using on-tissue trypsinization (MSMS data are consistent with the presence of two isomeric hybrid *N*-glycan isomers)

Figure S12. Product ion spectrum of $[M+Na]_+$ at *m/z* 1835.93, in permethylated glycans collected from porcine urothelium using on-tissue trypsinization (MSMS data are consistent with the presence of two isomeric *N*-glycan structures)

Figure S13. H&E and immunolabeling images of porcine bladders (histological evidence of urothelial removal without damage to the underlying tissue)

Figure S14. MALDI mass spectra of *N*-glycan profiles obtained from whole cell lysates of urothelia from three individual porcine bladders, (A) Uro1, (B) Uro2 and (C) Uro3 (mass spectra of analyses of whole urothelial cell lysates from three different animal bladders)

Figure S15. The relative percentages of *N*-glycans from whole cell lysates of urothelia from three independent porcine bladders, Uro1, Uro2, and Uro3 (average relative percentages and proposed glycan structures are presented)

Figure S16 Venn diagram showing the distribution of the 46 *N*-glycans from whole cell lysates of urothelia over three different porcine bladders

Table S1. 47 porcine urothelial cell apical surface *N*-glycans common to the three biological replicates (table summarizing mass spectrometric data for the 47 apical *N*-glycans common to the three replicate bladders)

Table S2. Table giving standard deviations and CVs for the 47 porcine urothelial cell apical surface *N*-glycans common to the three biological replicates

Table S3. 12 porcine urothelial cell apical surface O-glycans common to the three biological replicates (table summarizing the mass spectrometric data for the 12 apical O-glycans common to the three replicate bladders)

Table S4. Table giving standard deviations and CVs for the 12 porcine urothelial cell apical surface O-glycans common to the three biological replicates

Table S5. List of 29 urothelial total cell lysate *N*-glycans released by FANGS that were common to the three porcine bladders (table summarizing the mass spectrometric data from the 29

urothelial total cell lysate *N*-glycans common to the three individual bladders from which the urothelial cells were obtained)

AUTHOR INFORMATION

Corresponding Author

*Corresponding author: Jennifer Southgate +44 1904 328705 j.southgate@york.ac.uk;

Author contact information: Chung-Yao Wang CYWang20142018@gmail.com; Ed Bergström ed.bergstrom@york.ac.uk; Jane Thomas-Oates jane.thomas-oates@york.ac.uk

Author Contributions

The manuscript was written through contributions of all authors, as follows: JT-O., JS, and C-YW designed research; C-YW performed research; C-YW, EB, JS, JT-O analyzed data; JT-O., JS. and C-YW wrote the paper. All authors have given approval to the final version of the manuscript.

‡These authors contributed equally.

ACKNOWLEDGMENT

The authors are grateful to Dr Daniel Ungar for helpful discussions and his glycobiology insight throughout the development of this study. Dr Ashley Ward is thanked for his expert contribution to the design of the bladder stretch device described herein. We gratefully acknowledge the

assistance of Timothy Ayers (Electronics Workshop, Department of Chemistry, University of York) for his technical expertise with fabricating the reaction device for stretching and sampling bladder surfaces. Dr Jenny Hinley and Mrs Rosalind Duke of the Jack Birch Unit are thanked for their expert technical support with cell biological and immunohistochemical aspects of the study.

The York Centre of Excellence in Mass Spectrometry was created thanks to a major capital investment through Science City York, supported by Yorkshire Forward with funds from the Northern Way Initiative, and subsequent support from EPSRC (EP/K039660/1; EP/M028127/1).

JS and other members of the Jack Birch Unit receive support from York Against Cancer.

For TOC only

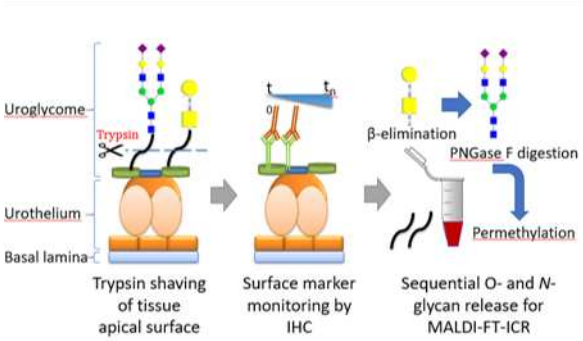

Declaration: The authors confirm that the TOC graphic is original, created by the authors, and has not been published elsewhere.

REFERENCES

1. Hamouda, H.; Kaup, M.; Ullah, M.; Berger, M.; Sandig, V.; Tauber, R.; Blanchard, V., Rapid analysis of cell surface N-glycosylation from living cells using mass spectrometry. *J Proteome Res* **2014,** 13, (12), 6144-51.
2. Mun, J. Y.; Lee, K. J.; Seo, H.; Sung, M. S.; Cho, Y. S.; Lee, S. G.; Kwon, O.; Oh, D. B., Efficient adhesion-based plasma membrane isolation for cell surface N-glycan analysis. *Anal Chem* **2013,** 85, (15), 7462-70.
3. Reinke, S. O.; Bayer, M.; Berger, M.; Blanchard, V.; Hinderlich, S., Analysis of Cell Surface N-glycosylation of the Human Embryonic Kidney 293T Cell Line. *J Carbohydr Chem* **2011,** 30, (4-6), 218-232.
4. Raghunathan, R.; Sethi, M. K.; Zaia, J., On-slide tissue digestion for mass spectrometry based glycomic and proteomic profiling. *MethodsX* **2019,** 6, 2329-2347.
5. Hu, P.; Meyers, S.; Liang, F.-X.; Deng, F.-M.; Kachar, B.; Zeidel, M.; Sun, T.-T., Role of membrane proteins in permeability barrier function uroplakin ablation elevate urothelial permeability. *Am J Physiol Renal Physiol* **2002,** 283, 1200-1207.
6. Hu, C. C.; Liang, F. X.; Zhou, G.; Tu, L.; Tang, C. H.; Zhou, J.; Kreibich, G.; Sun, T. T., Assembly of urothelial plaques: tetraspanin function in membrane protein trafficking. *Mol Biol Cell* **2005,** 16, (9), 3937-50.
7. Katnik-Prastowska, I.; Lis, J.; Matejuk, A., Glycosylation of uroplakins. Implications for bladder physiopathology. *Glycoconj J* **2014,** 31, (9), 623-36.
8. Nishiyama, T.; Matsumoto, Y.; Watanabe, H.; Fujiwara, M.; Sato, S., Detection of Tn antigen with vicia villosa agglutinin in urinary bladder cancer Its relevance to the patients clinical course. *J Natl Cancer Inst* **1987,** 78, 1113-1118.
9. Wu, X.-R.; Sung, T.-T.; Medina, J. J., In vitro binding of type 1-fimbriated Escherichia coli to uroplakins Ia and Ib Relation to urinary tract infections. *Proc. Natl. Acad. Sci USA* **1996,** 93, 9630-9635.
10. Xie, B.; Zhou, G.; Chan, S. Y.; Shapiro, E.; Kong, X. P.; Wu, X. R.; Sun, T. T.; Costello, C. E., Distinct glycan structures of uroplakins Ia and Ib: structural basis for the selective binding of FimH adhesin to uroplakin Ia. *J Biol Chem* **2006,** 281, (21), 14644-53.
11. Zhou, G.; Mo, W.-J.; Sebbel, P.; Min, G.; Neubert, T. A.; Glockshuber, R.; Wu, X.-R.; Sun, T.-T.; Kong, X.-P., 2001_Uroplakin Ia is the urothelial receptor for uropathogenic Escherichia coli evidence from in viro FimH binding. *J Cell Sci* **2001,** 114, 4095-4103.
12. Buckley, M.; Xin, P.; Washington, S.; Herb, N.; Erickson, D.; Bhavanandan, V. P., Lectin histochemical examination of rabbit bladder glycoproteins and characterization of a mucin isolated from the bladder mucosa. *Arch Biochem Biophys* **2000,** 375, (2), 270-7.
13. Higuch, T.; Xin, P.; Buckley, M. S.; Erickson, D. R.; Bhavanadan, V. P., Characterization of the rabbit homolog of human MUC1 glycoprotein isolated from bladder by affinity chromatography on immobilzed jacalin. *Glycobiology* **2000,** 10, (7), 659-667.
14. Hurst, R. E., Structure, function, and pathology of proteoglycans and glycosaminoglycans in the urinary tract. *World J Urol* **1994,** 12, 3-10.
15. Janssen, D. A.; van Wijk, X. M.; Jansen, K. C.; van Kuppevelt, T. H.; Heesakkers, J. P.; Schalken, J. A., The distribution and function of chondroitin sulfate and other sulfated glycosaminoglycans in the human bladder and their contribution to the protective bladder barrier. *J Urol* **2013,** 189, (1), 336-42.

16. Buckley, M. S.; Washington, S.; Laurent, C.; Erickson, D. R.; Bhavanadan, V. P., Characterization and immunohistochemical localization of the glycoconjugates of the rabbit bladder mucosa. *Arch Biochem Biophys* **1996,** 330, (1), 163-173.
17. Rodriguez-Ortega, M. J.; Norais, N.; Bensi, G.; Liberatori, S.; Capo, S.; Mora, M.; Scarselli, M.; Doro, F.; Ferrari, G.; Garaguso, I.; Maggi, T.; Neumann, A.; Covre, A.; Telford, J. L.; Grandi, G., Characterization and identification of vaccine candidate proteins through analysis of the group A Streptococcus surface proteome. *Nat Biotechnol* **2006,** 24, (2), 191-7.
18. Castro-Borges, W.; Dowle, A.; Curwen, R. S.; Thomas-Oates, J.; Wilson, R. A., Enzymatic shaving of the tegument surface of live schistosomes for proteomic analysis: a rational approach to select vaccine candidates. *PLoS Negl Trop Dis* **2011,** 5, (3), e993.
19. Montacir, H.; Freyer, N.; Knospel, F.; Urbaniak, T.; Dedova, T.; Berger, M.; Damm, G.; Tauber, R.; Zeilinger, K.; Blanchard, V., The Cell-Surface N-Glycome of Human Embryonic Stem Cells and Differentiated Hepatic Cells thereof. *Chembiochem* **2017,** 18, (13), 1234-1241.
20. Turner, A.; Subramanian, R.; Thomas, D. F.; Hinley, J.; Abbas, S. K.; Stahlschmidt, J.; Southgate, J., Transplantation of autologous differentiated urothelium in an experimental model of composite cystoplasty. *Eur Urol* **2011,** 59, (3), 447-54.
21. Wezel, F.; Pearson, J.; Southgate, J., Plasticity of in vitro-generated urothelial cells for functional tissue formation. *Tissue Eng Part A* **2014,** 20, (9-10), 1358-68.
22. Wada, Y.; Azadi, P.; Costello, C. E.; Dell, A.; Dwek, R. A.; Geyer, H.; Geyer, R.; Kakehi, K.; Karlsson, N. G.; Kato, K.; Kawasaki, N.; Khoo, K. H.; Kim, S.; Kondo, A.; Lattova, E.; Mechref, Y.; Miyoshi, E.; Nakamura, K.; Narimatsu, H.; Novotny, M. V.; Packer, N. H.; Perreault, H.; Peter-Katalinic, J.; Pohlentz, G.; Reinhold, V. N.; Rudd, P. M.; Suzuki, A.; Taniguchi, N., Comparison of the methods for profiling glycoprotein glycans--HUPO Human Disease Glycomics/Proteome Initiative multi-institutional study. *Glycobiology* **2007,** 17, (4), 411-22.
23. Abdul Rahman, S.; Bergstrom, E.; Watson, C. J.; Wilson, K. M.; Ashford, D. A.; Thomas, J. R.; Ungar, D.; Thomas-Oates, J. E., Filter-aided N-glycan separation (FANGS): a convenient sample preparation method for mass spectrometric N-glycan profiling. *J Proteome Res* **2014,** 13, (3), 1167-76.
24. Skeene, K.; Walker, M.; Clarke, G.; Bergstrom, E.; Genever, P.; Ungar, D.; Thomas-Oates, J., One Filter, One Sample, and the N- and O-Glyco(proteo)me: Toward a System to Study Disorders of Protein Glycosylation. *Anal Chem* **2017,** 89, (11), 5840-5849.
25. Loo, T.; Patchett, M. L.; Norris, G. E.; Lott, J. S., Using secretion to solve a solubility problem: high-yield expression in Escherichia coli and purification of the bacterial glycoamidase PNGase F. *Protein Expr Purif* **2002,** 24, (1), 90-8.
26. Dell, A.; Carman, N. H.; Tiller, P. R.; Thomas-Oates, J. E., Fast atom bombardment mass spectrometric strategies for characterizing carbohydrate-containing biopolymers. *Biomed Environ Mass Spectrom* **1988,** 16, (1-12), 19-24.
27. Dell, A.; Thomas-Oates, J. E., FAB-MS: Sample preparation and analytical strategies. In *Analysis of Carbohydrates by Gas Liquid Chromatography and Mass Spectrometry*, Biermann, C. J.; McGinnis, G. D., Eds. CRC: 1989; pp 217-235.
28. Ciucanu, I.; Kerek, F., A simple and rapid method for the permethylation of carbohydrates. *Carbohydr Res* **1984,** 131, 209-217.
29. Ceroni, A.; Maass, K.; Geyer, H.; Geyer, R.; Dell, A.; Haslam, S. M., GlycoWorkbench: a tool for the computer-assisted annotation of mass spectra of glycans. *J Proteome Res* **2008,** 7, (4), 1650-9.

30. Yang, G.; Tan, Z.; Lu, W.; Guo, J.; Yu, H.; Yu, J.; Sun, C.; Qi, X.; Li, Z.; Guan, F., Quantitative glycome analysis of N-glycan patterns in bladder cancer vs normal bladder cells using an integrated strategy. *J Proteome Res* **2015,** 14, (2), 639-53.
31. Korossis, S.; Bolland, F.; Southgate, J.; Ingham, E.; Fisher, J., Regional biomechanical and histological characterisation of the passive porcine urinary bladder: Implications for augmentation and tissue engineering strategies. *Biomaterials* **2009,** 30, (2), 266-75.
32. Rademaker, G. J.; Pergantis, S. A.; Blok-Tip, L.; Langridge, J. I.; Kleen, A.; Thomast-Oates, J. E., 1998_Mass Spectrometric Determination of the Sites of O-Glycan Attachment with Low Picomolar Sensitivity. *Anal Biochem* **1998,** 257, (257), 149-160.
33. Packer, N. H.; Lawson, M. A.; Jardine, D. R.; Redmond, J. W., A general approach to desalting oligosaccharides released from glycoproteins. *Glycoconjugate J* **1998,** 15, 737-747.
34. Loke, I.; Packer, N. H.; Thaysen-Andersen, M., Complementary LC-MS/MS-Based N-Glycan, N-Glycopeptide, and Intact N-Glycoprotein Profiling Reveals Unconventional Asn71-Glycosylation of Human Neutrophil Cathepsin G. *Biomolecules* **2015,** 5, (3), 1832-54.
35. Heiskanen, A.; Hirvonen, T.; Salo, H.; Impola, U.; Olonen, A.; Laitinen, A.; Tiitinen, S.; Natunen, S.; Aitio, O.; Miller-Podraza, H.; Wuhrer, M.; Deelder, A. M.; Natunen, J.; Laine, J.; Lehenkari, P.; Saarinen, J.; Satomaa, T.; Valmu, L., Glycomics of bone marrow-derived mesenchymal stem cells can be used to evaluate their cellular differentiation stage. *Glycoconj J* **2009,** 26, (3), 367-84.
36. Cross, W. R.; Eardley, I.; Leese, H. J.; Southgate, J., A biomimetic tissue from cultured normal human urothelial cells: analysis of physiological function. *Am J Physiol Renal Physiol* **2005,** 289, (2), F459-68.
37. Engles, C. D.; Hauser, P. J.; Abdullah, S. N.; Culkin, D. J.; Hurst, R. E., Intravesical chondroitin sulfate inhibits recruitment of inflammatory cells in an acute acid damage "leaky bladder" model of cystitis. *Urology* **2012,** 79, (2), 483 e13-7.
38. Hauser, P. J.; Buethe, D. A.; Califano, J.; Sofinowski, T. M.; Culkin, D. J.; Hurst, R. E., Restoring barrier function to acid damaged bladder by intravesical chondroitin sulfate. *J Urol* **2009,** 182, (5), 2477-82.
39. Hurst, R. E.; Roy, J. B.; Min, K. W.; Veltri, R. W.; Marley, G.; Patton, K.; Shackelford, D. L.; Stein, P.; Parsons, C. L., A deficit of chonroitin sulfate proteoglycans on the bladder urothelium in interstitial cystitis. *Urology* **1996,** 48, 817-821.
40. Nickel, J. C.; Downey, J.; Morales, A.; Emerson, L.; Clark, J., Relative efficacy of various exogenous glycosaminoglycans in providing a bladder surface permeability barrier. *J Urol* **1998,** 160, 612-614.
41. Parsons, C. L.; Stauffer, C.; Schmidt, J. D., Bladder-surface glycosaminoglycans: an efficient mechanism of environmental adaptation. *Science* **1980,** 208, (4444), 605-7.
42. An, H. J.; Gip, P.; Kim, J.; Wu, S.; Park, K. W.; McVaugh, C. T.; Schaffer, D. V.; Bertozzi, C. R.; Lebrilla, C. B., Extensive determination of glycan heterogeneity reveals an unusual abundance of high mannose glycans in enriched plasma membranes of human embryonic stem cells. *Mol Cell Proteomics* **2012,** 11, (4), M111 010660.
43. Malagolini, N.; Cavallone, D.; Wu, X.-R.; Serafini-Cessi, F., Terminal glycosylation of bovine uroplakin III, one of the major integral-membrane glycoproteins of mammalian bladder. *Biochim Biophys* **2000,** 1475, 231-237.
44. Tu, L.; Kong, X. P.; Sun, T. T.; Kreibich, G., Integrity of all four transmembrane domains of the tetraspanin uroplakin Ib is required for its exit from the ER. *J Cell Sci* **2006,** 119, (Pt 24), 5077-86.

45. Wu, X.-R.; Lin, J.-H.; Walz, T.; Häner, M.; Yu, J.; Aebi, U.; Sun, T.-T., Mammalian uroplakins. A group of highly conserved urothelial differentiation-related membrane proteins.pdf>. *J Biol Chem* **1994,** 269, 13716-13724.
46. Lin, J.-H.; Wu, X.-R.; Kreibich, G.; Sun, T.-T., Precursor sequence, processing and urothelium-specific expression of a major 15-kDa protein subunit of asymmetric unit membrane. *J Biol Chem* **1994,** 269, 1775-1784.
47. Yu, J.; Lin, J.-H.; Wu, X.-R.; Sun, T.-T., Uroplakins Ia and Ib, two major differentiation products of bladder epithelium belong to a family of four transmembrane domain (4TM) proteins. *J Cell Biol* **1994,** 125, 171-182.
48. Wellens, A.; Garofalo, C.; Nguyen, H.; Van Gerven, N.; Slattegard, R.; Hernalsteens, J. P.; Wyns, L.; Oscarson, S.; De Greve, H.; Hultgren, S.; Bouckaert, J., Intervening with urinary tract infections using anti-adhesives based on the crystal structure of the FimH-oligomannose-3 complex. *PLoS One* **2008,** 3, (4), e2040.
49. Desantis, S.; Accogli, G.; Zizza, S.; Arrighi, S., In situ characterization of glycans in the urothelium of donkey bladder: evidence of secretion of sialomucins. *Acta Histochem* **2013,** 115, (7), 712-8.
50. Limas, C.; Lang, P., T-antigen in normal and neoplastic urothelium. *Cancer* **1986,** 58, 1236-1245.
51. Mastrodonato, M.; Mentino, D.; Lopedota, A.; Cutrignelli, A.; Scillitani, G., A histochemical approach to glycan diversity in the urothelium of pig urinary bladder. *Microsc Res Tech* **2017,** 80, (2), 239-249.
52. N'Dow, J.; Jordan, N.; Robson, C. N.; Neal, D. E.; Pearson, J. P., The bladder does not appear to have a dynamic secreted continuous mucous gel layer. *J Urol* **2005,** 173, (6), 2025-31.
53. Nakagawa, T.; Uozumi, N.; Nakano, M.; Mizuno-Horikawa, Y.; Okuyama, N.; Taguchi, T.; Gu, J.; Kondo, A.; Taniguchi, N.; Miyoshi, E., Fucosylation of N-glycans regulates the secretion of hepatic glycoproteins into bile ducts. *J Biol Chem* **2006,** 281, (40), 29797-806.
54. Kinlough, C. L.; Poland, P. A.; Gendler, S. J.; Mattila, P. E.; Mo, D.; Weisz, O. A.; Hughey, R. P., Core-glycosylated mucin-like repeats from MUC1 are an apical targeting signal. *J Biol Chem* **2011,** 286, (45), 39072-81.
55. Mariño, K.; Bones, J.; Kattla, J. J.; Rudd, P. M., A systematic approach to protein glycosylation analysis: a path through the maze. *Nat Chem Biol* **2010,** 6, (10), 713-23.
56. Mulloy, B.; Dell, A.; Stanley, P.; J, H. P., Structural Analysis of Glycans. In *Essentials of Glycobiology*, Varki, A.; Cummings, R. D.; Esko, J. D.; Stanley, P.; Hart, G. W.; Aebi, M.; Darvill, A. G.; Kinoshita, T.; Packer, N. H.; Prestegard, J. H.; Schnaar, R. L.; Seeberger, P. H., Eds. Cold Spring Harbor Laboratory Press: Cold Spring Harbor (NY), 2015; pp 639-52.
57. Yang, X.; Bartlett, M. G., Glycan analysis for protein therapeutics. *J Chromatogr B Analyt Technol Biomed Life Sci* **2019,** 1120, 29-40.